Trop J Nat Prod Res, November 2025; 9(11): 5438 - 5446 **ISSN 2616-0684 (Print)**
ISSN 2616-0692 (Electronic)

Tropical Journal of Natural Product Research

Available online at https://www.tjnpr.org

Original Research Article

Green Synthesis of Silver Nanoparticles (AgNPs) using Cempedak *(Artocarpus champeden (Lour.) Stokes.)* Bark Extract: Evaluation of Anti-Inflammatory and Photodegradation Properties

Noor Hindryawati[1]*, Husna Syaima[1], Irfan Ashari Hiyahara[1], Teguh Wirawan[1], M. Syaiful Arief[1], Nanang Tri Widodo[1], Mega Silvia Dewi[1], Gaanty Pragas Maniam[2]

[1]*Department of Chemistry, Faculty of Mathematics and Natural Sciences, Mulawarman University, Samarinda, East Kalimantan, Indonesia*
[2]*Faculty of Industrial Sciences and Technology, Universiti Malaysia Pahang Al-Sultan Abdullah, Lebuhraya Tun Razak, Gambang, Kuantan, Pahang, Malaysia*

ARTICLE INFO

Article history:
Received 06 July 2025
Revised 13 October 2025
Accepted 17 October 2025
Published online 01 December 2025

ABSTRACT

Cempedak (*Artocarpus champeden*) bark, rich in flavonoids, phenolics, and alkaloids, was used as a natural bioreductant for the green synthesis of silver nanoparticles (AgNPs). In this context, microwave-assisted synthesis (450 W, 15–22 min) enabled rapid and uniform formation of stable AgNPs. Characterization using UV–Vis spectroscopy, particle size analysis (PSA), and transmission electron microscopy (TEM) also confirmed spherical nanoparticles with an average diameter of 69 nm. AgNPs synthesized at 22 minutes exhibited the highest absorbance and stability. Photocatalytic evaluation showed that 8% (v/v) AgNPs degraded 93.62% of 5 ppm methylene blue within 30 seconds, while anti-inflammatory assays reported 38.99% inhibition at 400 ppm (IC_{50} = 673.75 ppm), indicating moderate activity. These results showed that *A. champeden* bark extract served as an efficient and sustainable reducing agent for the production of bioactive and photocatalytically active AgNPs, offering potential applications in environmental remediation and biomedical fields.

Keywords: Silver nanoparticles, Cempedak Bark, Bioreductant, Anti-Inflammatory, Photodegradation.

Introduction

Nanotechnology has become a key multidisciplinary science with wide applications in medicine, environmental remediation, and materials engineering [1,2]. Among various nanomaterials, silver nanoparticles (AgNPs) have attracted remarkable attention because of the potent antimicrobial, catalytic, and optical properties [3-5]. These features enable the use in antimicrobial coatings, wastewater treatment, and drug delivery systems [6–8]. However, conventional synthesis methods frequently include toxic chemicals, high energy consumption, and long reaction times, which contradict the principles of sustainable nanotechnology [9,10]. Therefore, the development of rapid and eco-friendly methods for AgNP synthesis remains an important challenge. Green synthesis has been reported as a promising alternative that uses plant-derived biomolecules to act simultaneously as reducing and stabilizing agents[11,12]. Phytochemicals such as phenolics, flavonoids, and terpenoids can convert Ag^{+} ions into Ag^{0} nanoparticles while providing functional groups to enhance biocompatibility [13,14].

*Corresponding author. Email: hindryawati@gmail.com
Tel.: + 6285246646998

Citation: Hindryawati N, Syaima H, Hiyahara IA, Wirawan T, Arief MS, Widodo NT, Dewi MS, Maniam GP. Green Synthesis of Silver Nanoparticles (AgNPs) using Cempedak *(Artocarpus champeden (Lour.) Stokes.)* Bark Extract: Evaluation of Anti-Inflammatory and Photodegradation Properties. Trop J Nat Prod Res. 2025; 9(11): 5438 – 5446 https://doi.org/10.26538/tjnpr/v9i11.26

Official Journal of Natural Product Research Group, Faculty of Pharmacy, University of Benin, Benin City, Nigeria

This method avoids hazardous reagents and produces nanoparticles with improved biological activity [15,16]. Among the available green methods, microwave-assisted synthesis has received growing attention to ensure uniform heating, increase nucleation, and produce nanoparticles with controlled size and morphology [17,18]. Compared with conventional heating, microwave irradiation improves reaction kinetics and energy efficiency as an ideal strategy for large-scale green synthesis [19,20].

The *Artocarpus* genus, particularly *Artocarpus champeden* (Lour.) Stokes is rich in phenolic and flavonoid compounds with strong reducing potential [21,22]. Previous research has mostly explored the leaves or fruits of related species [23], while analyses using *A. champeden* bark as a bioreductant remain scarce despite the phytochemical richness. The presence of flavonoids, alkaloids, and phenolics in the bark extract suggests the potential for reducing and capping silver ions, obtaining nanoparticles with enhanced physicochemical and biological characteristics [24,25]. The efficiency of the degradation depends on the structure and size of AgNPs, as well as the interaction between the nanoparticles and the target organic compound [26]. Therefore, the development of AgNPs is environmentally friendly and effective in photocatalytic applications.

Based on the description, this research aimed to synthesize and characterize AgNPs using *A. champeden* bark extract as a natural bioreductant under microwave irradiation. Subsequently, the photocatalytic efficiency and anti-inflammatory activity of the synthesized nanoparticles were evaluated. The novelty of this research lies in the use of *A. champeden* bark as an underexplored phytochemical source for the rapid, green, and energy-efficient production of stable and bioactive AgNPs with dual environmental and biomedical potential.

Materials and Methods

Reagents and Chemicals

This research used several analytical-grade reagents and chemicals, these include methanol (Bendosen, 99.9%), Whatman filter paper (Sigma Aldrich), magnesium (Sigma Aldrich, 99%), hydrochloric acid (HCl, Sigma Aldrich, 37%), and ferric chloride ($FeCl_3$, Merck, 99%). Dragendorff's reagent (Sigma Aldrich), silver nitrate ($AgNO_3$, Merck, 99%), methylene blue (Biochemical, ≥98%), bovine serum albumin (BSA, Sigma Aldrich, >98%), Tris-buffered saline (TBS, Thermo Scientific, >98%), and diclofenac sodium (Rochem International).

Characterization

The formation of silver nanoparticles (AgNPs) was initially confirmed by UV–Vis spectroscopy (Thermo Scientific Orion AquaMate 8100) through the observation of characteristic surface plasmon resonance (SPR) peaks in the range of 400–450 nm. Absorbance was recorded over seven consecutive days to evaluate nanoparticle stability before further analyses. Particle size distribution was measured using a Nano Particle Analyzer SZ-100 (Horiba Ltd.), while morphology and particle aggregation were examined using Transmission Electron Microscopy (TEM, HITACHI HT7700, Japan).

Collection and Identification of Artocarpus champeden Stem Bark

Stem bark of *Artocarpus champeden* (cempedak) was collected on 22 June 2022 from the stem of a matured tree in Handil, Muara Jawa District, Kutai Kartanegara Regency, East Kalimantan, Indonesia (coordinates: ~0.748670° S, 117.266667° E). Furthermore, the specimen was authenticated by Mintoro Dwi Putra, S.Pd. (Laboratory of Anatomy and Plant Systematics, Faculty of Mathematics and Natural Sciences, Mulawarman University) and deposited in the herbarium (voucher no. 054/UN.17.8.5.7.16/HA/VI/2022). Bark samples were washed, air-dried at ambient room temperature of 27°C, cut into small pieces, and stored in a desiccator until extraction.

Extraction of Plant Materials

The extraction procedure was performed according to the method described by Lestari et al. [27] with slight modifications. A kilogram of dried bark powder was macerated with 3 L of methanol for three successive 24-hour cycles at room temperature (~27°C). The filtrates were combined and concentrated under reduced pressure using a rotary evaporator to obtain the crude methanolic extract, which was subjected to phytochemical screening.

Preliminary Phytochemical Screening

Qualitative phytochemical analysis was performed to identify secondary metabolites, including flavonoids, alkaloids, and phenolics [28]. Flavonoid detection was carried out by adding 1 mg of magnesium powder and three drops of concentrated hydrochloric acid to 1 mL of the extract, followed by vigorous shaking. The appearance of a red, yellow, or orange coloration showed the presence of flavonoids [28]. Alkaloids were also identified by adding two drops of Dragendorff's reagent to 1 mL of the extract. The formation of a brownish-orange precipitate was indicative of alkaloid compounds. In addition, phenolic compounds were detected by adding a few drops of 1% ferric chloride ($FeCl_3$) solution to 1 mL of the extract. The development of a black coloration confirmed the presence of phenolics [29].

Microwave-Assisted Synthesis of AgNPs

AgNPs were synthesized using a process developed by Tormena et al (2024) with modification [30]. In addition, 1.5 mM $AgNO_3$ solution was mixed with *A. champeden* bark extract in a 3:2 ratio (v/v). The reaction mixture was exposed to microwave irradiation at 450 W (Samsung ME731K/XSE) for 7–22 min. A colour change from pale yellow to brownish-yellow indicated the successful reduction of Ag^+ ions to metallic Ag^0 nanoparticles. After treatment, all samples were centrifuged for 10 minutes, and the obtained supernatants were analyzed using a UV-Visible spectrophotometer (Thermo Scientific Orion AquaMate 8100). The stability of the synthesized silver nanoparticles was assessed by recording UV–Vis absorption spectra daily for seven consecutive days.

Photocatalytic Activity

Degradation of Methylene Blue Using UV Light and Microwave Irradiation

Approximately two sets of 25 mL methylene blue (MB) solutions (5 ppm) were prepared in separate beakers. A total of 8% (v/v) of AgNPs was added relative to the total solution volume, and a set was exposed to ultraviolet (UV) irradiation using an 11-watt UV lamp for time intervals of 10, 20, 30, 40, 50, 60, and 90 min. The other set was subjected to microwave irradiation at 450 W for durations of 10, 20, 30, 60, 90, and 120 s. After treatment, the samples were centrifuged for 10 min, and the obtained supernatants were analyzed using a UV-Visible spectrophotometer (Thermo Scientific Orion AquaMate 8100) [31].

Variation of Reaction State

Aliquots (25 mL) of 5 ppm methylene blue solution were prepared with and without 8% (v/v) AgNPs and irradiated under microwaves (450 W, 30 s). The resulting mixtures were centrifuged for 10 min, and the absorbance of the supernatant was recorded by UV–Vis spectrophotometry (Thermo Scientific Orion AquaMate 8100) [31].

AgNPs and Methylene Blue Contact Time Variation

A mixture containing 25 mL of 5 ppm MB solution and 8% (v/v) AgNPs was irradiated under microwaves (450 W) for 10, 20, 30, 60, 90, and 120 s. After centrifugation for 10 min, absorbance was measured using a UV–Vis spectrophotometer [31].

Effect of Methylene Blue Concentration

In a beaker, 8% (v/v) AgNPs were added based on the volume of methylene blue. Furthermore, 25 mL of methylene blue solutions at concentrations of 1, 3, 5, 7, 9, and 10 ppm were introduced. The mixture was irradiated with microwave power at 450 W for 30 s, followed by centrifugation for 10 min. The obtained samples were analyzed using a UV-Vis spectrophotometer [31].

Effect in AgNPs Volume

In a separate set of experiments, 25 mL of a 5 ppm methylene blue solution was mixed with varying concentrations of AgNPs at 4%, 8%, 12%, 16%, and 22% (v/v). Each mixture was subjected to microwave irradiation for 30 s at a power of 450 W. After irradiation, the samples were centrifuged for 10 min and analyzed using a UV-Vis spectrophotometer [31].

Anti-Inflammatory Activity Assay

The anti-inflammatory activity was determined using the bovine serum albumin (BSA) denaturation method as described by reference [32].

Preparation of Bovine Serum Albumin (BSA) Solution in Tris Buffer Saline (TBS) and Negative Control Solution

A 0.2% (w/v) BSA solution was prepared in Tris-buffered saline (TBS, pH 7.4) by dissolving 0.2 g of BSA in TBS and adjusting the volume to 100 mL. For the negative control, approximately 500 µL of distilled water was transferred into a 5 mL volumetric flask, followed by the addition of the 0.2% BSA solution in TBS up to the calibration mark. The solution was incubated at 25 °C for 30 min and heated in a water bath at 72 °C for 5 min to induce protein denaturation. After cooling to room temperature of 27 °C for 25 min, absorbance was measured at 660 nm using a UV–Vis spectrophotometer, with TBS serving as the blank [32].

Preparation of Positive Control Solution

A stock solution of sodium diclofenac (1000 ppm) was prepared by dissolving 25 mg of the compound in distilled water and adjusting the volume to 25 mL in a volumetric flask. Subsequently, the solution was diluted using 0.2% BSA at concentrations of 100, 50, 25, 6.25, and 3.13 ppm. Each sample with the positive control was incubated in a water bath at 25 °C and 72 °C for 30 and 5 min, respectively. The samples were allowed to cool at room temperature (~27°C) for 25 min before measuring absorbance at 660 nm using a UV-Vis spectrophotometer and TBS as the blank [32].

ISSN 2616-0684 (Print)
ISSN 2616-0692 (Electronic)

Anti-Inflammatory Activity Test

Water was added to a concentration of 1000 ppm after the introduction of 25 mg of AgNPs to a 25 mL volumetric flask. The solution was diluted to achieve concentrations of 800, 600, 400, and 200 ppm using 0.2% BSA. Incubation was conducted for 30 min at 25 °C, followed by a 5-heating period in a water bath at 72 °C. After cooling to room temperature (~27°C) for 25 min, the absorbance was measured using a UV-Vis spectrophotometer set to a wavelength of 600 nm [32].

Results and Discussion

Phytochemical Screening of AgNPs

Approximately 1 kg of cempedak *(Artocarpus champeden (Lour.) Stokes.)* bark powder was extracted using methanol as the solvent through a maceration process. The resulting filtrate was concentrated with a rotary evaporator to obtain 202.2 g of crude extract (20.22% yield). Phytochemical screening of the extract (Table 1) confirmed the presence of secondary metabolites, including flavonoids, phenolics, and alkaloids. These phytochemicals are known to possess strong reducing and capping capabilities, facilitating nanoparticle formation [33–35]. In particular, phenolic compounds exhibit strong nucleophilic and electron-donating properties, enabling the reduction of Ag^{+} ions to metallic Ag^{0} and the stabilization of the resulting AgNPs through coordination with surface functional groups.

Table 1: Phytochemicals Test Results of Cempedak Bark Phytoconstituents

	Test
Flavonoids	+
Phenolics	+
Alkaloids	+

Description: (+) Contains secondary metabolites

The synthesis of AgNPs was carried out by reacting 1.5 mM $AgNO_3$ with 1% (m/v) cempedak bark extract as a bioreductant. The reaction was performed under microwave irradiation (450 W) for varying durations (7, 10, 12, 15, 18, 20, and 22 min) to accelerate the formation of AgNPs while maintaining the integrity of the phytochemical constituents [36,37]. Microwave-assisted synthesis offers uniform volumetric heating, shorter reaction time, and improved nucleation, which promote controlled nanoparticle growth without damaging thermolabile bioactive molecules. The characteristic surface plasmon resonance (SPR) of AgNPs was monitored using UV–Vis spectroscopy in the range of 400–425 nm. The reaction mixture exhibited a distinct colour change from colorless to brownish-yellow, confirming the reduction of Ag^{+} to Ag^{0} and the formation of colloidal AgNPs (Figure 2). There was no significant SPR absorption during the initial 7–12 min, indicating incomplete reduction. The development of a sharp peak at 420 nm between 15 and 22 min confirmed the nucleation and growth of AgNPs, with the highest absorbance recorded after 22 min of irradiation. Therefore, AgNPs synthesized for 22 min were selected as optimal due to the higher absorbance and greater reaction completion. The colour change and corresponding spectral behavior corroborated the formation of stable silver nanoparticles.

Optical Stability and Particle Size Analysis of AgNPs

The temporal stability of AgNPs was evaluated using UV–Vis spectrophotometry over seven days (Figure 3). The sample synthesized for 22 min exhibited the most stable SPR peak with minimal wavelength shift, while shorter synthesis times (15–20 min) showed slight red shifts (420–440 nm) and fluctuating absorbance values, indicating particle aggregation and instability. The stable peak position and colour retention (brownish hue maintained after seven days, Figure 4) confirmed the colloidal stability of AgNPs. The hydroxyl (–OH) and carbonyl groups in the phytoconstituents served as reducing and capping agents, forming an electrostatic double layer around AgNPs and preventing agglomeration through steric stabilization.

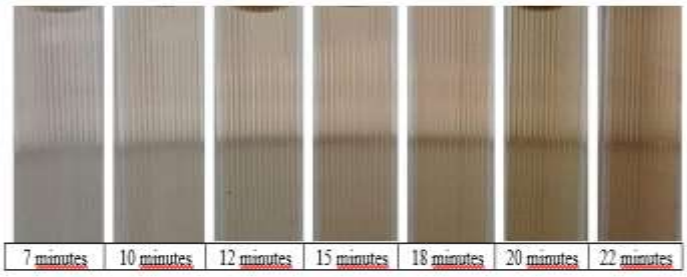

Figure 1: Visual observation of colour changes during the synthesis of silver nanoparticles (AgNPs) at different reaction times (7–22 minutes).

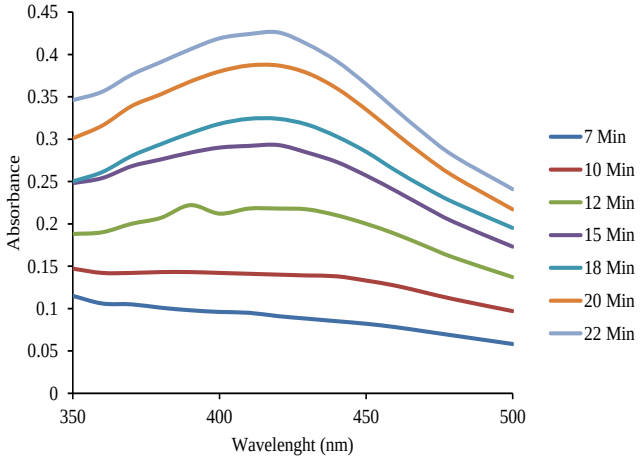

Figure 2: Maximum wavelength measurement results of AgNPs based on synthesis time variation

Particle size analysis (PSA) revealed that the AgNPs had an average hydrodynamic diameter of 68.9 nm with a distribution range of 15–250 nm (Figure 5). The first peak (15–40 nm) was attributed to primary nanoparticles, whereas the broader secondary peak (65–250 nm) suggested the presence of aggregated species. Despite the broader range, the mean size of 68.9 nm indicated a relatively uniform and stable particle distribution. Such minor variations in size are commonly associated with partial agglomeration during biosynthesis, which is strongly influenced by extract composition and reaction duration.

Transmission electron microscopy (TEM) analysis confirmed that the synthesized AgNPs were predominantly spherical with moderate size uniformity (Figure 6). The diameter was computed to estimate the particle size distribution using ImageJ software, with an average diameter of 67.95 nm, consistent with PSA data (68.9 nm) (Figure 7). The close agreement between measurements validated the synthesis consistency and reliability. The morphological features showed that the phytochemicals successfully mediated reduction and stabilization, leading to nanoscale particles suitable for catalytic and biological applications.

Photocatalytic Activity

Comparative research of UV and microwave irradiation effects on AgNPs synthesis

The photocatalytic efficiency of the synthesized AgNPs was assessed by the degradation of methylene blue (MB) dye under UV and microwave irradiation (Figure 8). UV irradiation (11 W) and microwave irradiation (450 W) were used under separate conditions to examine comparative degradation kinetics. Under microwave exposure, 93.62% degradation of MB was achieved within 30 s, while only

ISSN 2616-0684 (Print)
ISSN 2616-0692 (Electronic)

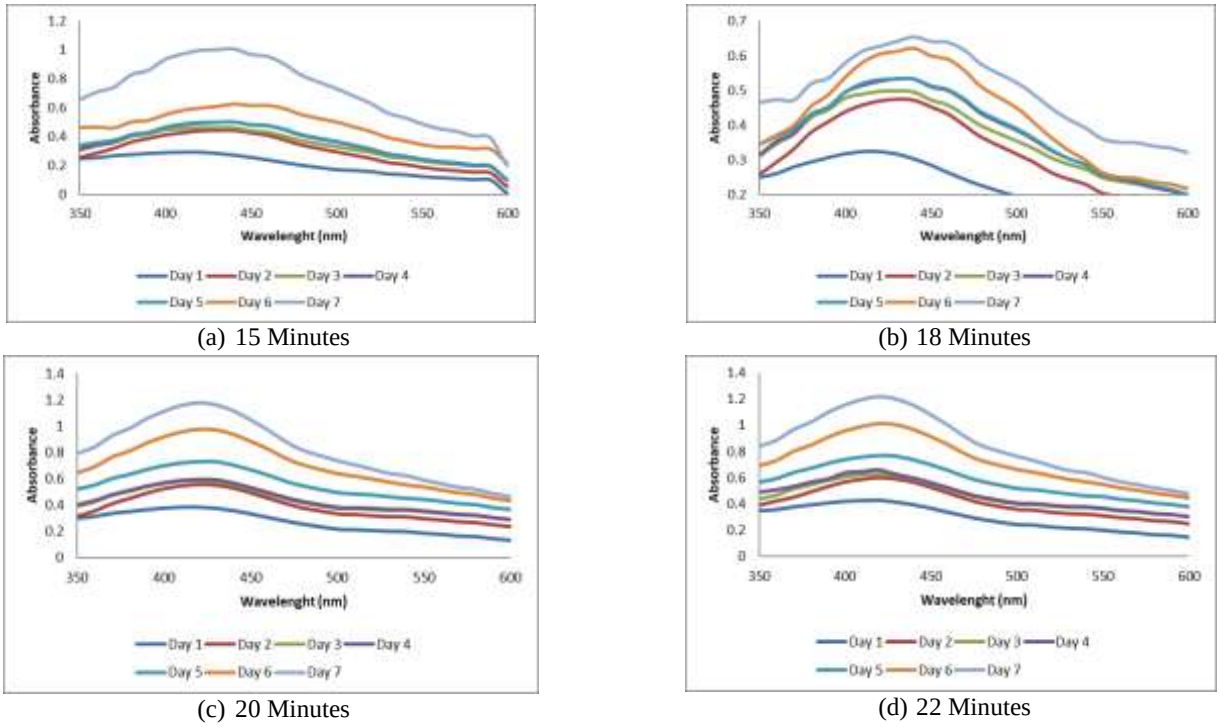

(a) 15 Minutes (b) 18 Minutes

(c) 20 Minutes (d) 22 Minutes

Figure 3: AgNPs stability observation result for 7 days, synthesis time (a) 15 minutes, (b) 18 minutes, (c) 20 minutes, and (d) 22 minutes

77.90% occurred after 90 min under UV light. The superior performance under microwave treatment was attributed to combined thermal and non-thermal effects that enhance molecular motion, collision frequency, and redox reactions [38]. The thermal effect ensures rapid and uniform heating, while the non-thermal effect enhances the rate of radical formation, leading to efficient degradation within a shorter period.

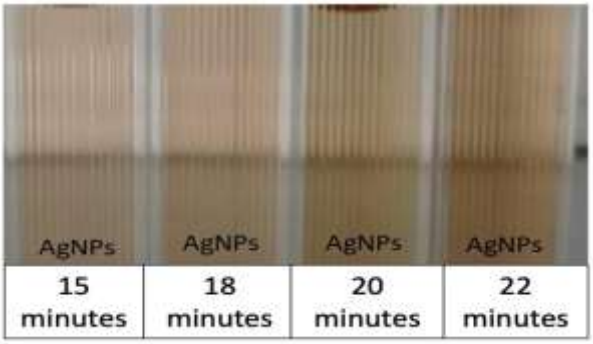

Figure 4: Visual observation of AgNPs synthesized at different reaction times (15–22 min), showing a colour change from light yellow to dark brown, indicating nanoparticle formation and growth due to surface plasmon resonance (SPR).

During photocatalysis, microwaves were used, resulting in a 20% increase in the production of O-H radicals. Therefore, the microwave-assisted degradation method maximized the duration of the methylene blue degradation process. The reaction treatment was conducted separately using microwaves and in combination with AgNPs to evaluate the effectiveness in degrading the methylene blue dye.

Figure 9 shows the relationship between photodegradation conditions and the degradation percentage. According to Figure 9, 59.52% degradation occurred when microwaves were not used and AgNPs were absent. This happened because heating a sample with microwaves created stationarity within the sample, enhancing the heating rate in higher energy areas. In this context, pollutants disintegrated in the aqueous phase when microwaves were directly irradiated on the effluent. The proportion of degradation increased to 93.62% when microwaves and AgNPs were added. This improvement occurred because the methylene blue dye degraded into simpler molecules through photon-induced photodegradation. Figure 9 shows the optimal conditions for methylene blue dye degradation under microwave-based settings with AgNPs.

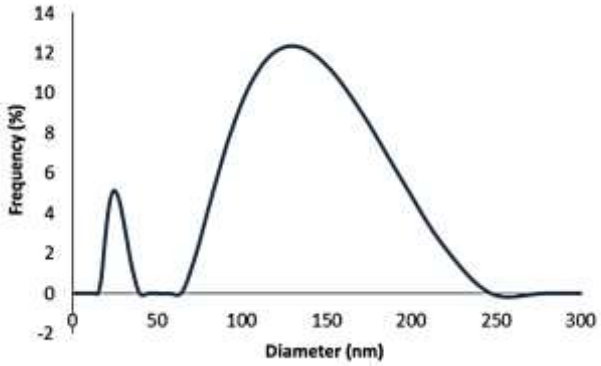

Figure 5: Particle size distribution of silver nanoparticles (AgNPs) with Cempedak Bark Extract as a bioreductant analyzed by Particle Size Analyzer (PSA).

AgNPs are an important type of catalyst required for photodegradation. The basic principle included exposure to light or energy, which causes electrons to move from the valence to the conduction band. This movement created holes, leading to the formation of OH radicals when water interacted with AgNPs. Furthermore, O_2 radicals were also created when electrons interact with air. These active radicals degraded organic substances into water, carbon dioxide, and mineral acids. Initially, the OH radical reacted with the C-S^+=C group, resulting in the formation of the sulfoxide group, C-S(=O)-C. The radicals reacted with the group, leading to the development of sulfones.

ISSN 2616-0684 (Print)
ISSN 2616-0692 (Electronic)

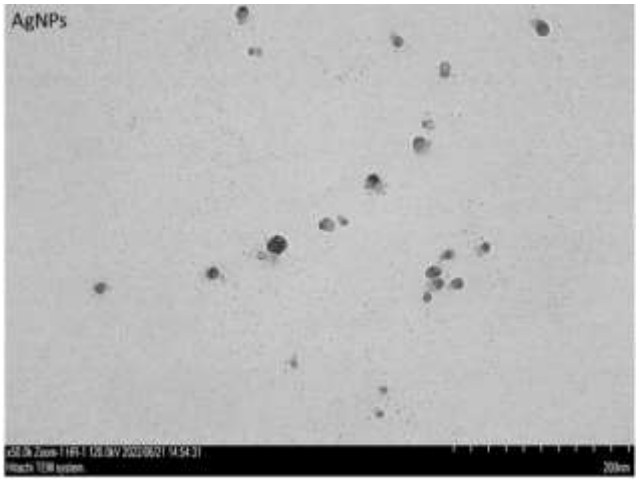

Figure 6: TEM image of AgNPs synthesized from 1.5 mM $AgNO_3$ and Cempedak bark extract (3:2 ratio), showing predominantly spherical nanoparticles with uniform distribution. Captured using Hitachi HT7700 at 120 kV and 50,000× magnification; scale bar = 200 nm.

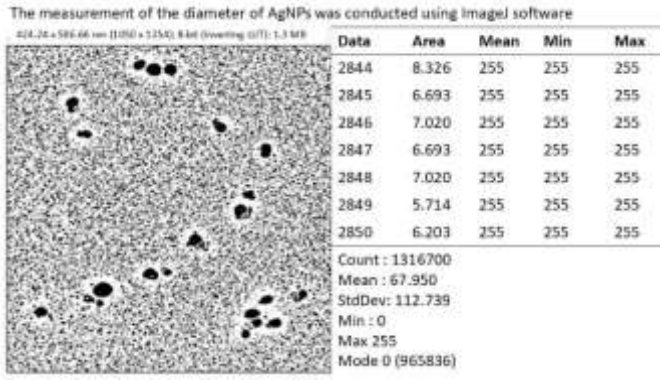

Figure 7: ImageJ analysis of silver nanoparticles (AgNPs) from TEM micrograph showing grayscale intensity distribution (Mean = 67.95; SD = 112.74; Count = 1,316,700; Max = 255), indicating a wide contrast range that represents well-dispersed AgNPs across the image. The mean and standard deviation values were obtained from ImageJ histogram analysis (Count = 1,316,700; Max intensity = 255), reflecting pixel intensity variation correlated with particle density and dispersion within the TEM image.

The group was targeted by OH radicals to release sulfonic acid. The oxidation process ceased when the state of sulfur reached the maximum. Additionally, the degradation of the nitrogen group in methylene blue included two processes. The central amino group had a double bond from N=C, occupying the space of the aromatic ring because the $-S^+ =$ group was broken. The OH radical, which generated a substituted aniline group, caused the saturation state of the amino bonds. The replaced amino group produced phenol and an NH_2 radical, yielding ammonia and ammonium. OH radicals also oxidized one methyl and two symmetric dimethyl phenyl amino groups to provide alcohol and aldehyde. An acid could facilitate reoxidation and decarboxylation, converting compounds into CO_2. The R- C_6H_4-$N(CH_3)_2$ group was also subjected to oxidation by the OH radical, leading to the formation of phenyl-methylamine. Aromatic rings participated in a hydroxylation reaction to make hydroxy hydroquinone and phenol molecules, while amino groups produced ammonium ions, which were oxidized to nitrate. The byproducts of methylene blue degradation included CO_2, SO_4^{2-}, NH_4^+, and NO_3^-.

Effect of Contact Time, MB Concentration, and AgNP Volume

The effect of contact time on photocatalytic efficiency was examined to determine the optimal exposure duration for methylene blue (MB) degradation by AgNPs. As shown in Figure 10, 25 mL of 5 ppm MB solution containing 8% (v/v) AgNPs was irradiated under microwave conditions for 10–120 s. The corresponding degradation efficiencies were 73.36%, 74.34%, 93.62%, 91.80%, 91.52%, and 90.12%, respectively. The rapid increase up to 30 s indicated sufficient generation of hydroxyl radicals (·OH) and effective photocatalytic activation, whereas shorter durations (10–20 s) resulted in incomplete degradation due to limited radical formation. Prolonged irradiation beyond 30 s produced no further improvement, suggesting that the reaction reached equilibrium once most dye molecules had been decomposed. Thus, 30 s was identified as the optimum contact time, confirming that microwave-assisted catalysis achieves rapid degradation within seconds compared with conventional minute-scale treatments.

The influence of MB concentration on photocatalytic performance is illustrated in Figure 11. The reaction was performed using 8% AgNPs (v/v) and varying MB concentrations (1–10 ppm) under microwave irradiation for 30 s. The degradation percentages were 67.20%, 62.00%, 93.62%, 61.72%, 63.23%, and 63.44%, respectively. The maximum efficiency (93.62%) occurred at 5 ppm, indicating that this concentration provided an optimal balance between dye availability and catalyst surface area. At lower concentrations (1–3 ppm), the reduced number of dye molecules limited ·OH radical generation and photon absorption, resulting in lower degradation rates. Conversely, at higher concentrations (≥ 7 ppm), the degradation efficiency decreased due to excessive dye loading, which caused light scattering and surface saturation of AgNPs, affecting active-site accessibility. These observations indicate that 5 ppm MB represents the optimal substrate concentration for efficient microwave-assisted photodegradation.

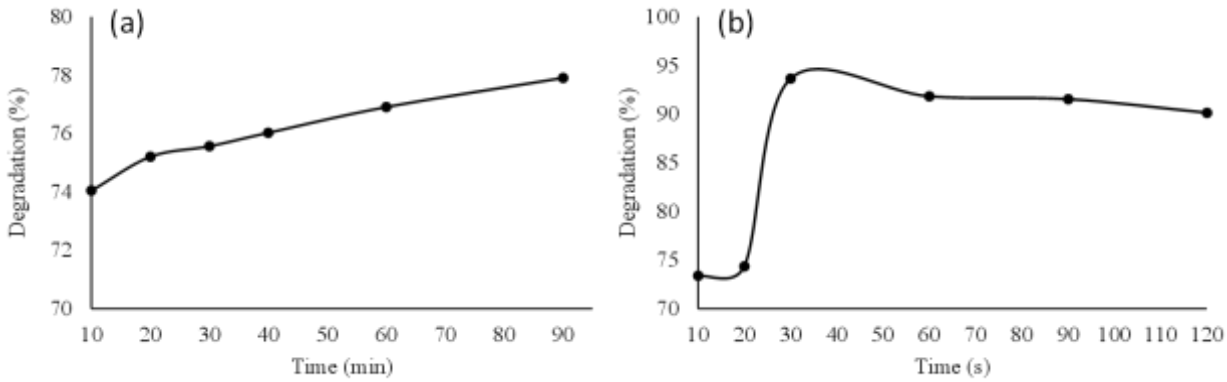

Figure 8: Comparison of photocatalytic activity at different reaction times under (a) UV irradiation and (b) microwave irradiation.

ISSN 2616-0684 (Print)
ISSN 2616-0692 (Electronic)

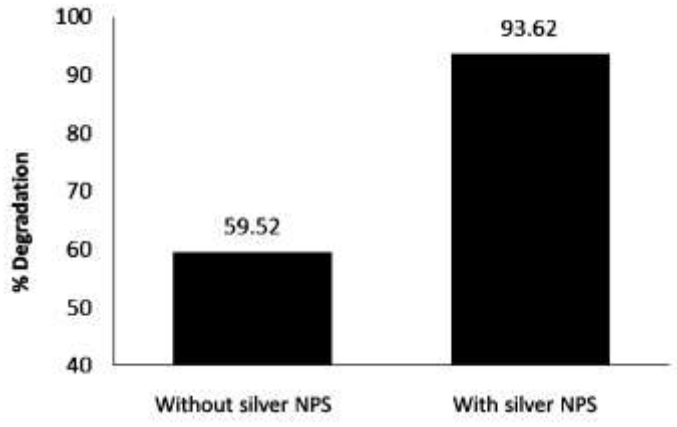

Figure 9: Microwave Assistance in Photodegradation Reaction with and without AgNPs

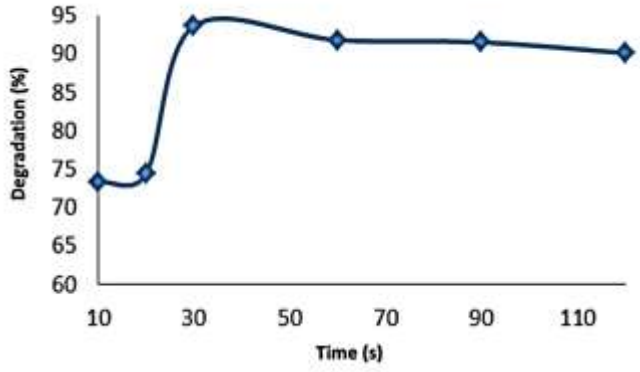

Figure 10: Effect of Contact Time on Methylene Blue Degradation by AgNPs

The effect of catalyst dosage on degradation efficiency was evaluated by varying the AgNPs volume from 4% to 22% (v/v) while maintaining 5 ppm MB and a 30 s irradiation time (Figure 12). The corresponding degradation efficiencies were 68.78%, 93.62%, 69.74%, 69.20%, 64.94%, and 60.28%, respectively. The results showed that increasing AgNPs loading up to 8% improved degradation due to the greater availability of catalytically active sites for radical generation. However, further increases beyond 8% led to a decline in performance caused by particle aggregation and excessive turbidity in the reaction medium, which reduced light penetration and effective photon utilization. Therefore, 8% (v/v) was determined to be the optimal catalyst loading, balancing surface area and optical transparency for maximum photocatalytic efficiency.

Overall, these results reported that optimal degradation efficiency (93.62%) was achieved using 5 ppm MB, 8% AgNPs, and a 30 s contact time under 450 W microwave irradiation. The superior efficiency and extremely short reaction time further confirm the synergistic influence of microwave irradiation and AgNP catalysis in promoting rapid and sustainable pollutant degradation.

Anti-Inflammatory Activity

The anti-inflammatory potential of the synthesized AgNPs was evaluated using the bovine serum albumin (BSA) denaturation assay, with sodium diclofenac serving as the positive control. Diclofenac, a well-established non-steroidal anti-inflammatory drug (NSAID), significantly inhibited protein denaturation even at 3.13 ppm, exhibiting 21.86% inhibition, surpassing the minimum activity threshold of 20%. These results are consistent with previous reports highlighting diclofenac's ability to stabilize protein structures under thermal stress.[39] Inhibition of protein denaturation is a widely accepted *in vitro* model for assessing anti-inflammatory activity in both synthetic drugs and bioactive natural products.

Figure 14 illustrates the anti-inflammatory performance of the bioreductant-mediated AgNPs. The AgNPs demonstrated concentration-dependent inhibition of protein denaturation, reaching 38.99% at 400 ppm, while the 200 ppm sample showed only 14.94% inhibition. The calculated IC_{50} value for AgNPs was 673.75 ppm, compared with 9.10 ppm for diclofenac sodium, indicating moderate but significant anti-inflammatory potential.

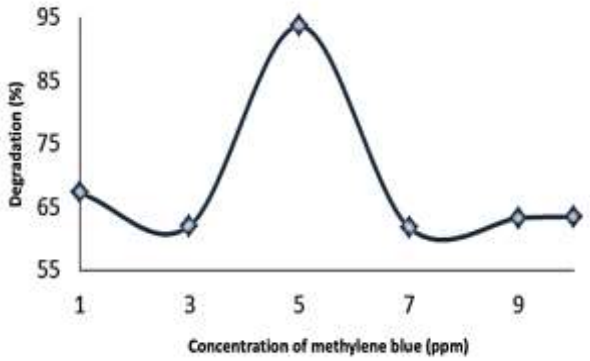

Figure 11: Photodegradation of methylene blue with various methylene blue concentrations

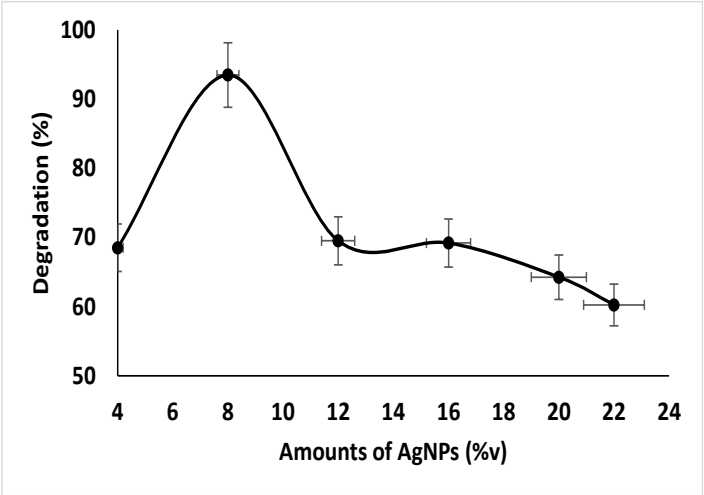

Figure 12: Effect of AgNPs volume on photocatalytic degradation. The highest degradation was observed at 8% (v/v) AgNPs. Error bars indicate standard deviation (n = 3).

The observed effect was attributed to the interaction between AgNPs and BSA molecules, where nanoparticles bind to polar amino acid residues, thereby preventing heat-induced unfolding and aggregation. The relatively small particle size and large surface area of AgNPs enhance these molecular interactions, contributing to the inhibitory activity. Although less potent than diclofenac, the AgNPs synthesized using *A. champeden* bark extract exhibited biologically relevant anti-inflammatory effects. The activity may stem from residual phytochemicals—such as flavonoids and phenolics—adsorbed on the nanoparticle surface, which can synergistically stabilize protein structures and suppress denaturation. These results highlight the multifunctional potential of the biosynthesized AgNPs, combining environmental remediation and moderate anti-inflammatory properties.

ISSN 2616-0684 (Print)
ISSN 2616-0692 (Electronic)

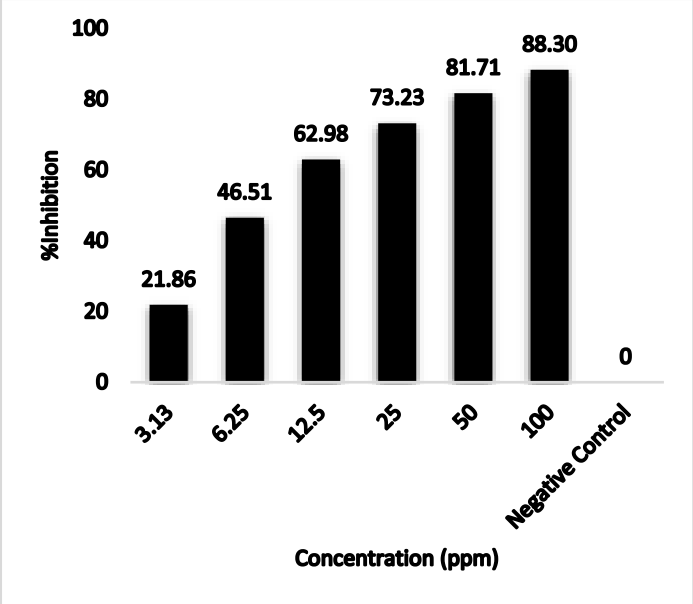

Figure 13: The result of natrium diclofenac sodium's anti-inflammatory activity (positive control)

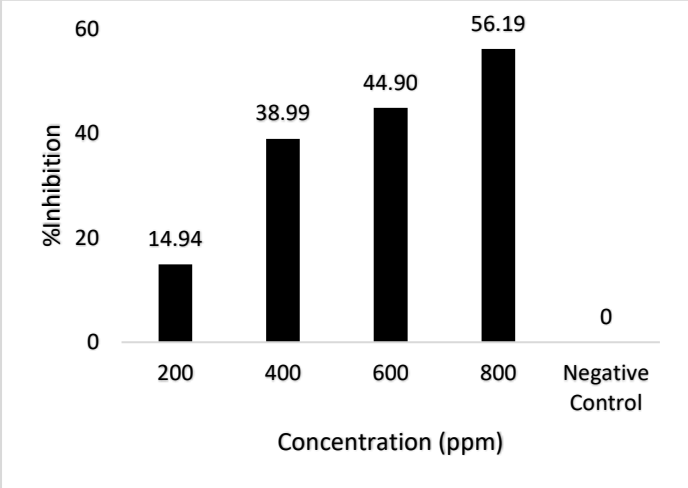

Figure 14: The results of the anti-inflammatory activity of AgNPs

Conclusion

This research successfully reported the rapid and eco-friendly synthesis of silver nanoparticles (AgNPs) using *Artocarpus champeden* bark extract as a natural bioreductant. The phytochemical constituents, particularly flavonoids and phenolics, played a crucial role as reducing and capping agents to obtain stable, spherical AgNPs with an average diameter of 68 nm. The microwave-assisted method significantly enhanced reaction efficiency, enabling nanoparticle formation within 22 minutes under mild conditions. The biosynthesized AgNPs exhibited excellent photocatalytic performance, achieving up to 93.62% degradation of methylene blue within only 30 second under 450 W microwave irradiation. Optimal conditions were observed at 5 ppm dye concentration, 8% AgNPs loading, and a 30-second exposure, confirming the synergistic effect between microwaves and the catalytic surface of AgNPs in generating reactive hydroxyl radicals. Furthermore, the nanoparticles displayed moderate anti-inflammatory activity, with an IC_{50} value of 673.75 ppm, attributed to the ability to stabilize protein conformation and the synergistic contribution of bioactive phytochemicals adsorbed on the nanoparticle surface. Overall, this work highlights the potential of *A. champeden*-derived AgNPs as sustainable, biocompatible, and multifunctional nanomaterials for environmental and biomedical applications. The integration of green synthesis and microwave-assisted catalysis provides a promising method for developing efficient and environmentally responsible nanotechnologies.

Conflict of Interest

The authors declare no conflict of interests.

Authors' Declaration

The authors hereby declare that the works presented in this article are original and that any liability for claims relating to the content of this article will be borne by them.

Acknowledgements

The authors are grateful to the Faculty of Mathematics and Natural Sciences, Mulawarman University, for funding this research under the 2023 PNBP Grant (1691/UN17.7/LT/2023).

References

1. Elzein B. Nano Revolution: Tiny tech, big impact: How nanotechnology is driving SDGs progress. Heliyon. 2024; 10:1-26. DOI: https://doi.org/10.1016/j.heliyon.2024.e31393
2. Akinniyi JN. Synthesis and characterization of copper nanoparticles using *Allium cepa* (L.) outer peel at ambient temperature. Trop J Nat Prod Res. 2025; 9(3):1144-1149. DOI: https://doi.org/10.26538/tjnpr/v9i3.32
3. Hochvaldová L, Panáček D, Válková L, Večeřová R, Kolář M, Prucek R, Kvitek L, Panacek A. *E. coli* and *S. aureus* resist AgNPs via an identical mechanism, but through different pathways. Commun Biol. 2024; 7:1-10. DOI: https://doi.org/10.1038/s42003-024-07266-3
4. Nandhini R, Rajeswari E, Harish S, Sivakumar V, Gangai SR, Jaya SD. Role of chitosan nanoparticles in sustainable plant disease management. J Nano Res. 2025; 27(13):1-35. DOI: https://doi.org/10.1007/s11051-024-06203-z
5. Mwangi NV, Madivoli SE, Kangogo M, Wangui MC, Wanakai IS, Nzilu MD, Waudo. An evaluation of the antimicrobial potency of AgNPs synthesised from *Fusarium sp*. Discov Appl Sci. 2024; 6(4):201. DOI: https://doi.org/10.1007/s42452-024-05870-w
6. Misra R, Hazra S, Saleem S, Nehru S. Drug-loaded polymer-coated AgNPs for lung cancer theranostics. Med Oncol. 2024; 41(6):132. DOI: https://doi.org/10.1007/s12032-024-02372-y
7. Sharma R, Tyagi S, Kandwal A, Bachheti RK, Bachheti A. Green synthesis of silver/silver chloride nanoparticles mediated by *Alternanthera philoxeroides* leaf extract and their biological activity. Russ J Gen Chem. 2024; 94(7):1750–1757. DOI: https://doi.org/10.1134/S1070363224070181
8. Pradhan L, Sah P, Nayak M, Upadhyay A, Pragya P, Tripathi S, Singh G, Maunika B, Paik P, Mukherjee S. Biosynthesized AgNPs prevent bacterial infection in the chicken egg model and mitigate biofilm formation on medical catheters. J Bio Inorg Chem. 2024; 29(3):353–373. DOI: https://doi.org/10.1007/s00775-024-02050-4
9. Yang S, Zhang C, Yong L, Niu M, Cheng W, Zhang L. Construction of PNIPAM/graphene oxide loaded with AgNPs interpenetrating intelligent hydrogels for antibacterial dressing. Polym Bull. 2024; 81(14):13027–13044. DOI: https://doi.org/10.1007/s00289-024-05274-1
10. Rehman F, Ali A, Zubair M, Waheed U, Khan R, Yaqoob A, Shahzadi I, Siddique M. Microwave-assisted green synthesis of AgNPs and chitosan nanocomposites for the removal of reactive blue-19. Int J Environ Sci Tech. 2025; 22(2):1001–1016. DOI: https://doi.org/10.1007/s13762-024-05674-w
11. Karpuz Ö, Baltacı C, Gül A, Gülen J, Bozbeyoğlu P, Aydoğan N. Green synthesis of iron and AgNPs from aqueous extract of buckwheat husk waste: antibacterial, cytotoxic, and dye

decolorization properties. Biomass Convers Biorefin. 2024. DOI: https://doi.org/10.1007/s13399-024-06287-6
12. Asefian S, Ghavam M. Green and environmentally friendly synthesis of AgNPs with antibacterial properties from some medicinal plants. BMC Biotechnol. 2024; 24(1):5. DOI: https://doi.org/10.1186/s12896-023-00828-z
13. Fabiani VA, Silvia D, Liyana D, Akbar H. Synthesis of Silver Nanoparticles Using Leaf Extract of *Cratoxylum glaucum* as a Bioreductant via Microwave Irradiation Method. Full J Chem. 2019; 4(2):96-101. DOI: https://doi.org/10.37033/fjc.v4i2.102
14. Punuri JB, Sharma P, Sibyala S, Tamuli R, Bora U. Piper betle-mediated green synthesis of biocompatible gold nanoparticles. Int Nano Lett. 2012; 2(1):18. DOI: https://doi.org/10.1186/2228-5326-2-18
15. Priya RS, Geetha D, Ramesh PS. Antioxidant activity of chemically synthesized AgNPs and biosynthesized Pongamia pinnata leaf extract mediated AgNPs – A comparative study. Ecotoxicol Environ Saf. 2016; 134:308–318. DOI: https://doi.org/10.1016/j.ecoenv.2015.07.037
16. Akhter MS, Rahman MA, Ripon RK, Mubarak M, Akter M, Mahbub S, Mahbub S, Mamun FA, Sikder MT. A systematic review on green synthesis of AgNPs using plant extracts and their biomedical applications. Heliyon. 2024; 10(11):e29766. DOI: https://doi.org/10.1016/j.heliyon.2024.e29766
17. Fabiani VA, Sutanti F, Silvia D, Putri MA. Green Synthesis of Silver Nanoparticles Using *Cratoxylum glaucum* Leaf Extract as a Bioreductant. IJoPAC. 2018; 1(2):68-76. DOI: https://doi.org/10.26418/indonesian.v1i2.30533
18. Hayaza S, Arifriandini HI, Malek NANN, Susilo RJK, Sajidah ES. Biosynthesis of Iron Oxide Nanoparticles Using Okra Pods Extract and Its Anticancer Activity on WiDr Colon Cancer Cells. Trop J Nat Prod Res. 2025; 6(9):2513–2518. DOI: https://doi.org/10.26538/tjnpr/v9i6.23
19. Ikhwan RM, Nurlely N, Fadlilaturrahmah F, Ma'shumah M. Phytochemical Screening and Determination of Total Phenolic Content in Leaf Extracts of *Artocarpus heterophyllus*, *Artocarpus integer*, and *Artocarpus odoratissimus* from Pengaron Village, Banjar Regency. J Insan Farmasi Indonesia. 2021; 4(1):95–102. DOI: https://doi.org/10.36387/jifi.v4i1.667
20. Hakim AR, Saputri R, Savitri AS, Ujuldah A, Sadlia F. Antioxidant Activity of Cempedak (*Artocarpus integer* (Thunb.) Merr.) Fruit Peel from South Kalimantan. J Surya Medika. 2022; 7(2):10–13. DOI: https://doi.org/10.33084/jsm.v7i2.2858
21. Fahim M, Shahzaib A, Nishat N, Jahan A, Bhat TA, Inam A. Green synthesis of AgNPs: A comprehensive review of methods, influencing factors, and applications. JCIS Open. 2024; 16: 100125. DOI: https://doi.org/10.1016/j.jciso.2024.100125
22. Sultana MstJ, Nibir AIS, Ahmed FRS. Biosensing and anti-inflammatory effects of silver, copper, and iron nanoparticles from the leaf extract of Catharanthus roseus. Beni-Suef Univ J Basic Appl Sci. 2023; 12(1): 26. DOI: https://doi.org/10.1186/s43088-023-00358-9
23. Mathesh A, Carmelin DS, Mohanprasanth A, Sravanthy PG, Snega R, Surya M, Saravana M. Tridax procumbens–mediated one-pot synthesis of silver-doped fucoidan nanoparticles and their antibacterial, antioxidant, and anti-inflammatory efficacy. Biomass Convers Biorefin. 2024; 14(8): 9887–9896. DOI: https://doi.org/10.1007/s13399-023-05265-8
24. Khan ZUR, Assad N, Naeem-ul-Hassan M, Sher M, Alatawi FS, Alatawi MS, Omran AME, Jame RMA, Adnan M, Khan MN, Ali B, Wahab S, Razale SA, Javed MA, Kaplan A, Rahimi M. Correction to: *Aconitum lycoctonum* L. (Ranunculaceae) mediated biogenic synthesis of AgNPs as potential antioxidant, anti-inflammatory, antimicrobial, and antidiabetic agents. BMC Chem. 2023; 17(1): 143. DOI: https://doi.org/10.1186/s13065-023-01058-2
25. Ristianingsih Y, Istiani A, Irfandy F. Equilibrium Study of Methylene Blue Adsorption onto Fe_2O_3-Impregnated Activated Carbon Derived from Corncob. J Teknol Agro-Ind. 2020; 7(1): 47–55. DOI: https://doi.org/10.34128/jtai.v7i1.115
26. Boddu S, Kondiboina N, Sandeep J, Vivek K, Prasad MB, Srinu N, Subbaiah T. Green AgNPs: A Sustainable Approach for Photocatalytic Degradation of Rhodamine B. J Ins Eng. (India): D. 2024; 105(3): 1989–1997. DOI: https://doi.org/10.1007/s40033-023-00621-4
27. Lestari A, Prince S, Jusniar. Isolation and Identification of Secondary Metabolites from the Chloroform Extract of Breadfruit (*Artocarpus altilis*) Stem Bark. J Chem. 2016; 17(1). 76-82. DOI: https://doi.org/10.35580/chemica.v17i1.4572
28. Lumowa SVT, Bardin S. Phytochemical Screening of Kepok Banana (*Musa paradisiaca* L.) as a Natural Source of Botanical Pesticide with Potential to Suppress Insect Pests in Short-Lived Crops. J Sains Kes. 2018; 1(9): 445-469. DOI: https://doi.org/10.25026/jsk.v1i9.87
29. Rahmayani LPD, Edyson, Budiarti LY. Comparison of Antibacterial Activity between Single and Combined Infusions of *Phyllanthus niruri* and *Peperomia pellucida* against *Escherichia coli.* Homeostatis. 2020; 3(1): 67-74. DOI: https://doi.org/10.20527/ht.v3i1.2017
30. Tormena RPI, Santos M-KMS, Silva AO, Félix FM, Chaker JA, Freire DO, Silva ICR, Moya SE, Sausa MH. Enhancing the antimicrobial activity of AgNPs against pathogenic bacteria by using *Pelargonium sidoides* DC extract in microwave-assisted green synthesis. RSC Adv. 2024; 14(30): 22035–22043. DOI: https://doi.org/10.1039/D4RA04140B
31. Shaikh WA, Chakraborty S, Islam RU. Photocatalytic Degradation of Rhodamine B Under UV Irradiation Using *Shorea robusa* Leaf Extract-Mediated Bio-Synthesis AgNPs. Int J Environ Sci Technol. 2019. DOI: https://doi.org/10.1007/s13762-019-02473-6
32. Farida Y, Rahmat D, Amanda AW. Anti-Inflammation Activity Test of Nanoparticles Ethanol Extract of *Temulawak Rhizome (Curcuma xanthorrhiza Roxb.)* with Protein Denaturation Inhibition Method. Ind J Pharm Sci. 2018; 16(2): 225. DOI: https://doi.org/10.35814/jifi.v16i2.569
33. Ayad R, Akkal S. Phytochemistry and biological activities of *algerian Centaurea* and related genera. Stud Nat Prod Chem. 2019; 63: 357–414. DOI: https://doi.org/10.1016/B978-0-12-817901-7.00012-5
34. Bandara N, Chalamaiah M. Bioactives from Agricultural Processing By-products. Encycl Food Chem. 2019; 472–480. DOI: https://doi.org/10.1016/B978-0-08-100596-5.22408-6
35. Negi AS, Jain S. Recent advances in natural product-based anticancer agents. Stud Nat Prod Chem. 2022; 75: 367–447. DOI: https://doi.org/10.1016/B978-0-323-91250-1.00010-0
36. Langa F, De La CP, De La HA, Diaz-Ortiz A, Diez-Barra E. Microwave Irradiation: More Than Just a Method for Accelerating Reactions. ChemInform. 1998; 29(1). DOI: https://doi.org/10.1039/CO9970400373
37. Bao C, Serrano-Lotina A, Niu M, Portela R, Li Y, Lim KH, Liu P, Wan W-J, Banares MA, Wang Q. Microwave-associated chemistry in environmental catalysis for air pollution remediation: A review. Chem Eng J. 2023; 466: 142902. DOI: https://doi.org/10.1016/j.cej.2023.142902
38. Jung SC. The microwave-assisted photo-catalytic degradation of organic dyes. Water Sci Technol. 2011; 63(7): 1491–1498. DOI: https://doi.org/10.2166/wst.2011.393
39. Gunathilake KDPP, Ranaweera KKDS, Rupasinghe HPV. Influence of Boiling, Steaming, and Frying of Selected Leafy Vegetables on the In Vitro Anti-Inflammation Associated Biological Activities. Plants. 2018; 7(1): 22. DOI: https://doi.org/10.3390/plants7010022